






Article

Synthesis, X-ray Structure and Hirshfeld Surface Analysis of Zn(II) and Cd(II) Complexes with s-Triazine Hydrazone Ligand

Saied M. Soliman ^{1,*}, Ayman El-Faham ¹, Assem Barakat ², Alexandra M. Z. Slawin ³,
John Derek Woollins ^{3,4} and Morsy A. M. Abu-Youssef ^{1,*}

¹ Department of Chemistry, Faculty of Science, Alexandria University, P.O. Box 426, Ibrahimia, Alexandria 21321, Egypt; ayman.elfaham@alexu.edu.eg or aymanel_faham@hotmail.com

² Department of Chemistry, College of Science, King Saud University, P.O. Box 2455, Riyadh 11451, Saudi Arabia; ambarakat@ksu.edu.sa

³ School of Chemistry, University of St Andrews, St Andrews KY16 9ST, UK; amzs@st-andrews.ac.uk (A.M.Z.S.); jdww3@st-andrews.ac.uk (J.D.W.)

⁴ Department of Chemistry, Khalifa University, Abu Dhabi 999041, United Arab Emirates

* Correspondence: saied1soliman@yahoo.com or saeed.soliman@alexu.edu.eg (S.M.S.); morsy5@alexu.edu.eg (M.A.M.A.-Y.)

Abstract: The two group IIB complexes [Cd(DMPT)Cl₂] (**6**) and [Zn(DMPT)Cl₂] (**7**) of the tridentate ligand (DMPT), 2,4-bis(morpholin-4-yl)-6-[(E)-2-[1-(pyridin-2-yl) ethylidene]hydrazin-1-yl]-1,3,5-triazine were synthesized, and their structural aspects were elucidated with the aid of X-ray crystallography. Both complexes crystallized in the monoclinic crystal system, with *P*2₁/*n* as a space group. The unit cell parameters for **6** are *a* = 14.1563(9) Å, *b* = 9.4389(6) Å, *c* = 16.5381(11) Å and β = 91.589(5)° while the respective values for **7** are 11.3735(14), 13.8707(13), 14.9956(16), and 111.646(2)°. The unit cell volume is slightly less (2198.9(4) Å³) in complex **7** compared to complex **6** (2209.0(2) Å³). Both complexes have a penta-coordination environment around the metal ion, where the DMPT ligand acts as a neutral tridentate NNN-chelate via the pyridine, hydrazone, and one of the s-triazine N-atoms. The penta-coordination environment of the Cd(II) in complex **6** is close to a square pyramidal configuration with some distortion. On the other hand, the ZnN₃Cl₂ coordination environment is highly distorted and located intermediately between the trigonal bipyramidal and square pyramids. Supramolecular structure analysis of **6** with the aid of Hirshfeld calculations indicated the importance of the Cl...H, O...H, and C...H interactions. Their percentages were calculated to be 20.9, 9.1, and 8.7%, respectively. For **7**, the Cl...H, O...H, C...H, and N...H contacts are the most important. Their percentages are 20.3, 9.0, 7.0, and 8.4%, respectively. In both complexes, the major intermolecular interaction is the hydrogen-hydrogen interactions which contributed 45.5 and 46.6%, respectively.

Keywords: group IIB; 1,3,5-triazine; X-ray crystallography; supramolecular structure; hirshfeld topology



Citation: Soliman, S.M.; El-Faham, A.; Barakat, A.; Slawin, A.M.Z.; Woollins, J.D.; Abu-Youssef, M.A.M. Synthesis, X-ray Structure and Hirshfeld Surface Analysis of Zn(II) and Cd(II) Complexes with s-Triazine Hydrazone Ligand. *Crystals* **2023**, *13*, 1232. <https://doi.org/10.3390/cryst13081232>

Academic Editors: Valerian Dragutan, Ileana Dragutan, Fu Ding and Ya-Guang Sun

Received: 5 July 2023

Revised: 26 July 2023

Accepted: 7 August 2023

Published: 10 August 2023



Copyright: © 2023 by the authors. Licensee MDPI, Basel, Switzerland. This article is an open access article distributed under the terms and conditions of the Creative Commons Attribution (CC BY) license (<https://creativecommons.org/licenses/by/4.0/>).

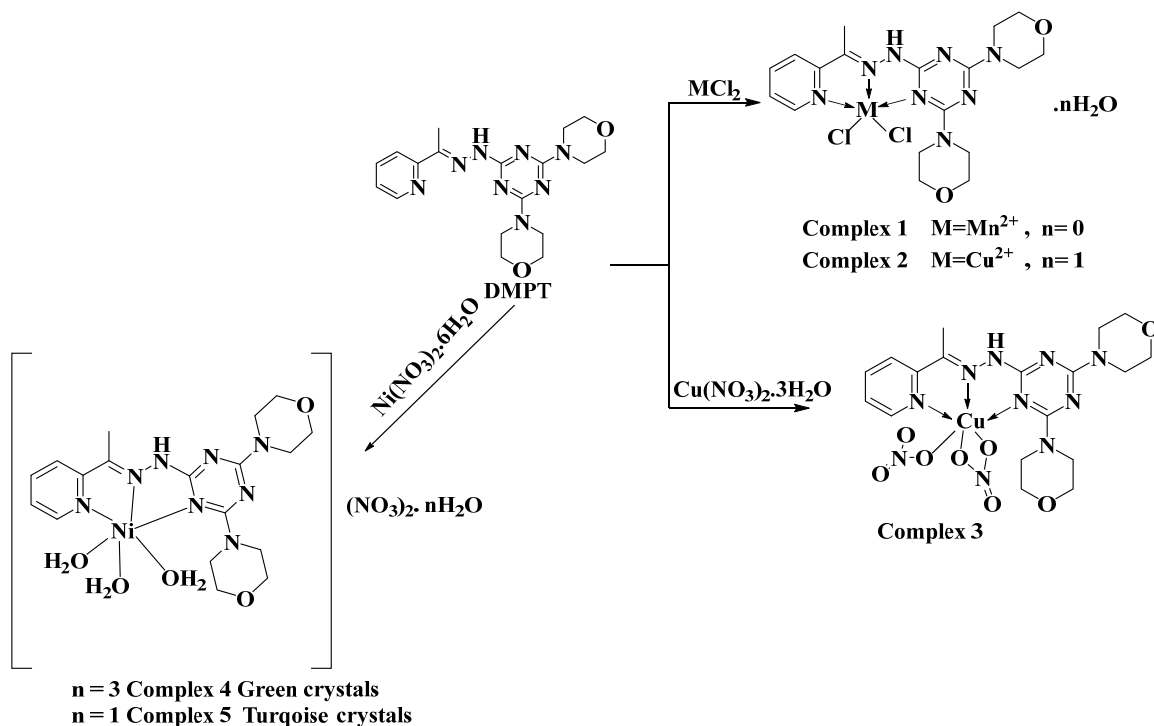
1. Introduction

s-Triazine ligands are an important class of organic compounds that not only have diverse uses in the field of pharmaceutical chemistry but are also employed as smart materials in coordination chemistry to construct metal-organic hybrids with interesting molecular and supramolecular architectures [1]. These metal-organic hybrids have diverse properties, which allow their use in different fields where the nature of the ligands' binding sites has great importance for their chelation power and also for their functional properties. In this regard, nitrogen heterocyclic compounds, including their Schiff base derivatives, are extensively reported as powerful chelating agents in the field of coordination chemistry [2–6].

In particular, Schiff bases have exhibited a broad range of applications, including coordination chemistry, pigments and dyes, industrial food, catalysis transformation, chemosensors, polymer stabilizers, and as synthons in organic synthesis for many biologically active compounds [6]. The imine or azomethine group, as the main functionality of

the Schiff bases, seems to play a critical role in a broad range of pharmacological applications. In addition, Schiff base metal complexes have been developed and have received a lot of attention in the last decade due to their electroluminescent effects and many pharmacological activities, including urease inhibitors, anti-fungal, anti-bacterial, anti-viral, anti-apoptotic potentials, DNA-binding efficacy, and as intermediates of pharmaceutically active cocrystals, which additionally showed remarkable NLO (nonlinear optical) and fluorescence applications. Schiff bases have also been employed in the application of organic photovoltaic compounds, sensors, and polymeric materials [6]. Specifically, Schiff base-based s-triazazine ligands are among this attractive class of organic compounds and were found attractive by many researchers [1]. This class of organic compounds was utilized as chelating ligands with many metal ions and also showed exciting biological activities.

Zn(II) and Cd(II) metal ions have flexible coordination environments and could form metal complexes with diverse coordination numbers. Many Zn(II) and Cd(II) complexes with Schiff bases and s-triazazine ligands were reported in the literature [7–15]. As a representative example, Ş. Uysal and coworkers designed, characterized, and explored the magnetic properties of star-shaped metal complexes with triazine core Schiff base ligands [16]. S. R. Kala reported the synthesis, NLO, and biological activities of metal (II) complexes with s-triazazine-based ligands [17]. Also, the El-Faham research group reported the synthesis, biological activity (antimicrobial and anticancer) of a new Cd (II) pincer complex with a s-triazazine core ligand [18]. Recently, the same research group designed novel s-triazazine-cored Schiff base ligands, exploring their coordination behavior as well as their biological activity with different divalent metal ions, including Ni (II), Mn(II), and Cu(II) metal centers [19,20]. In all cases, the s-triazazine-cored Schiff base ligands are found to be NNN-tridentate chelates, leading to different complexes with coordination numbers that depend on the metal ion (Scheme 1). In addition, the studied ligand has a morpholino substituent in addition to the aromatic s-triazazine core. This morpholine moiety has a number of C-H bonds that could form C-H... π and Cl...H intermolecular interactions. These non-covalent forces could play an important role in the supramolecular structure of the target complexes.



Scheme 1. Synthesis of the previously reported metal(II) complexes with 2,4-bis(morpholin-4-yl)-6-[(E)-2-[1-(pyridin-2-yl) ethylidene]hydrazin-1-yl]-1,3,5-triazine (DMPT).

Supramolecular chemistry is a promising field in chemistry that deals with molecular systems in which the molecules are connected together by weak non-covalent interactions. Supramolecular chemistry is important for medical diagnostic sensors [21,22], maintenance-free materials [23,24], and molecular encapsulation [25,26]. Supramolecular chemistry is included in everyday items, medicine, sensors, materials, and extraction technologies [27]. In the light of the diverse applications of group IIB complexes and in continuation of our previous work with this class of s-triazine-cored Schiff base ligands, as well as in order to explore their coordination chemistry and diverse coordination behavior towards different metal ions, we reported herein the synthesis and characterization using X-ray crystallography, including supramolecular structure investigations with the aid of Hirshfeld surface analysis, for the Zn(II) and Cd(II) complexes with the same s-triazines ligand (DMPT).

2. Materials and Methods

2.1. Physical Measurements

All the chemicals were bought from Sigma-Aldrich and used without additional purification. CHN analyses were carried out using a PerkinElmer 2400 Elemental Analyzer. The metal content was determined with the aid of a Shimadzu atomic absorption spectrophotometer (AA-7000 series, Shimadzu, Ltd., Tokyo, Japan). FTIR spectra were recorded at the Central Lab, Faculty of Science, Alexandria University, using a Bruker Tensor 37 FTIR spectrophotometer (Bruker Company, Karlsruhe, Germany) in KBr pellets at 4000–400 cm^{-1} (Figures S1–S3; Supplementary Data).

2.2. Preparation of DMPT

The DMPT was prepared following the procedure reported in our previous work [19].

2.3. Synthesis of Complexes [Cd(DMPT)Cl₂] (6) and [Zn(DMPT)Cl₂] (7)

An ethanolic solution of the organic ligand DMPT (115.2 mg, 0.3 mmol in 15 mL) was mixed with an aqueous solution of CdCl₂ (55.0 mg, 0.3 mmol in 5 mL) or ZnCl₂ (40.9 mg, 0.3 mmol in 5 mL). The clear mixtures were left at room temperature for a couple of days to slowly evaporate. The complexes [Cd(DMPT)Cl₂] (6) and [Zn(DMPT)Cl₂] (7) were obtained as colorless crystals after five days. The target crystals were collected from solutions and were found suitable for the X-ray single crystal structure measurement.

Complex 6, Anal. Calc. C₁₈H₂₄CdCl₂N₈O₂: C, 38.08; H, 4.26; N, 19.74; Cd, 19.80%. Found: C, 37.83; H, 4.15; N, 19.67; Cd, 19.71%. IR (KBr, cm^{-1}): 3443 ν (N–H), 2965, 2898 ν (C–H), 1595, 1574 ν (C=N), 1504 ν (C=C), 1257 ν (C–N).

Complex 7, Anal. Calc. C₁₈Cl₂N₈O₂ZnH₂₄: C, 41.52; H, 4.65; N, 21.52; Zn, 12.56%. Found: C, 41.24; H, 4.54; N, 21.38; Zn, 12.39%. IR (KBr, cm^{-1}): 3446 ν (N–H), 2964, 2910 ν (C–H), 1601, 1568 ν (C=N), 1502 ν (C=C), 1256 ν (C–N).

2.4. X-ray Crystallography

The experimental X-ray crystallographic measurements [28] are provided in the Supplementary Materials. Crystal data for complexes 6 and 7 is presented in Table 1.

Table 1. Crystal data for complexes 6 and 7.

Identification Code	6	7
CCDC	2278824	22788245
Empirical formula	C ₁₈ H ₂₄ CdCl ₂ N ₈ O ₂	C ₁₈ Cl ₂ N ₈ O ₂ ZnH ₂₄
Formula weight	567.76	520.73
Temperature/K	173	173
Crystal system	monoclinic	monoclinic
Space group	P2 ₁ /n	P2 ₁ /c

Table 1. Cont.

Identification Code	6	7
a/Å	14.1563(9)	11.3735(14)
b/Å	9.4389(6)	13.8707(13)
c/Å	16.5381(11)	14.9956(16)
$\alpha/^\circ$	90	90
$\beta/^\circ$	91.589(5)	111.646(2)
$\gamma/^\circ$	90	90
Volume/Å ³	2209.0(2)	2198.9(4)
Z	4	4
$\rho_{\text{calc}}/\text{g}/\text{cm}^3$	1.707	1.573
μ/mm^{-1}	1.265	1.393
F(000)	1144	1072
Crystal size/mm ³	0.14 × 0.14 × 0.04	0.1 × 0.1 × 0.03
Radiation	Mo K α ($\lambda = 0.71075$)	Mo K α ($\lambda = 0.71075$)
2 Θ range for data collection/ $^\circ$	3.736 to 54.97	3.852 to 50.754
Index ranges	$-18 \leq h \leq 18, -12 \leq k \leq 12, -21 \leq l \leq 21$	$-13 \leq h \leq 13, -16 \leq k \leq 16, -18 \leq l \leq 18$
Reflections collected	22180	26947
Independent reflections	5062 [$R_{\text{int}} = 0.0579, R_{\text{sigma}} = 0.0407$]	4028 [$R_{\text{int}} = 0.0220, R_{\text{sigma}} = 0.0126$]
Data/restraints/parameters	5062/1/285	4028/0/285
Goodness-of-fit on F^2	1.007	1.087
Final R indexes [$I \geq 2\sigma(I)$]	$R_1 = 0.0300, wR_2 = 0.0768$	$R_1 = 0.0204, wR_2 = 0.0597$
Final R indexes [all data]	$R_1 = 0.0456, wR_2 = 0.0822$	$R_1 = 0.0220, wR_2 = 0.0602$
Largest diff. peak/hole/e Å ⁻³	0.97/−0.73	0.44/−0.34

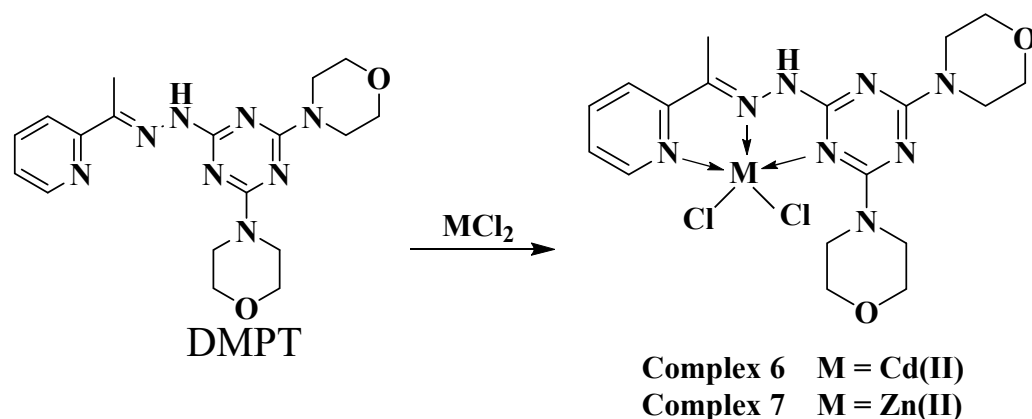
2.5. Hirshfeld Surface Analysis

The Crystal Explorer Ver. 3.1 program [29] was used to perform this analysis.

3. Results and Discussion

3.1. Synthesis and Characterizations

The self-assembly of the organic ligand (DMPT) [19,20] with different metal(II) salts was reported by our research team. The reaction of this ligand with Ni(NO₃)₂·6H₂O afforded two hexa-coordinated Ni(II) complexes [Ni(DMPT)(NO₃)₂]·3H₂O; **4** and [Ni(DMPT)(NO₃)₂]·H₂O; **5**, which have a very similar coordination environment but differ in the number of hydration water molecules (Scheme 1). Using Cu(NO₃)₂·6H₂O as a metal salt, the isolated crystals were found to be the hexa-coordinated [Cu(DMPT)(NO₃)₂] complex **3**. On the other hand, the reaction of CuCl₂ and MnCl₂ with the same ligand using the same reaction conditions afforded the penta-coordinated complexes [Mn(DMPT)Cl₂]; **1** and [Cu(DMPT)Cl₂]·H₂O; **2** (Scheme 1). Both complexes were found to have a distorted trigonal bipyramidal configuration around the metal(II) center. In this work, the reaction of DMPT with the group IIB metal salts CdCl₂ and ZnCl₂ afforded the [Cd(DMPT)Cl₂] and [Zn(DMPT)Cl₂] complexes as colorless, high-quality crystals, respectively. Their structures were confirmed using elemental analysis, FTIR spectroscopy, and X-ray crystallography (Scheme 2). FTIR data for DMPT, **6** and **7** are presented in Figure S1 (Supplementary Data). The most significant variations in the FTIR of complexes **6** and **7** compared to that for DMPT occurred in the $\nu_{(\text{C}=\text{N})}$ vibrations. The bands detected at 1595 and 1574 cm⁻¹ in **6** and 1601 and 1568 in **7** are assigned to the $\nu_{(\text{C}=\text{N})}$ vibrations. The corresponding values in DMPT are 1523 and 1492 cm⁻¹, respectively. Hence, the coordination between the DMPT and the metal ions Zn(II) and Cd(II) shifts the $\nu_{(\text{C}=\text{N})}$ modes to higher wavenumbers. Additionally, both structures were determined using X-ray crystallography.



Scheme 2. Synthesis of complexes 6 and 7.

3.2. X-ray Structure Description

The structure of the heteroleptic complex $[\text{Cd}(\text{DMPT})\text{Cl}_2]$ (**6**) was proved unambiguously using single-crystal X-ray diffraction. The $[\text{Cd}(\text{DMPT})\text{Cl}_2]$ complex crystallized in the monoclinic crystal system and $P2_1/n$ as a space group. The unit cell parameters are $a = 14.1563(9) \text{ \AA}$, $b = 9.4389(6) \text{ \AA}$, $c = 16.5381(11) \text{ \AA}$ and $\beta = 91.589(5)^\circ$. The asymmetric formula of this complex contains one $[\text{Cd}(\text{DMPT})\text{Cl}_2]$ formula. In the unit cell, there are four $[\text{Cd}(\text{DMPT})\text{Cl}_2]$ units, where the unit cell volume is $2209.0(2) \text{ \AA}^3$, while the calculated density is 1.707 mg/m^3 . The presentation of the coordination sphere of the $[\text{Cd}(\text{DMPT})\text{Cl}_2]$ complex (**6**) is shown in Figure 1.

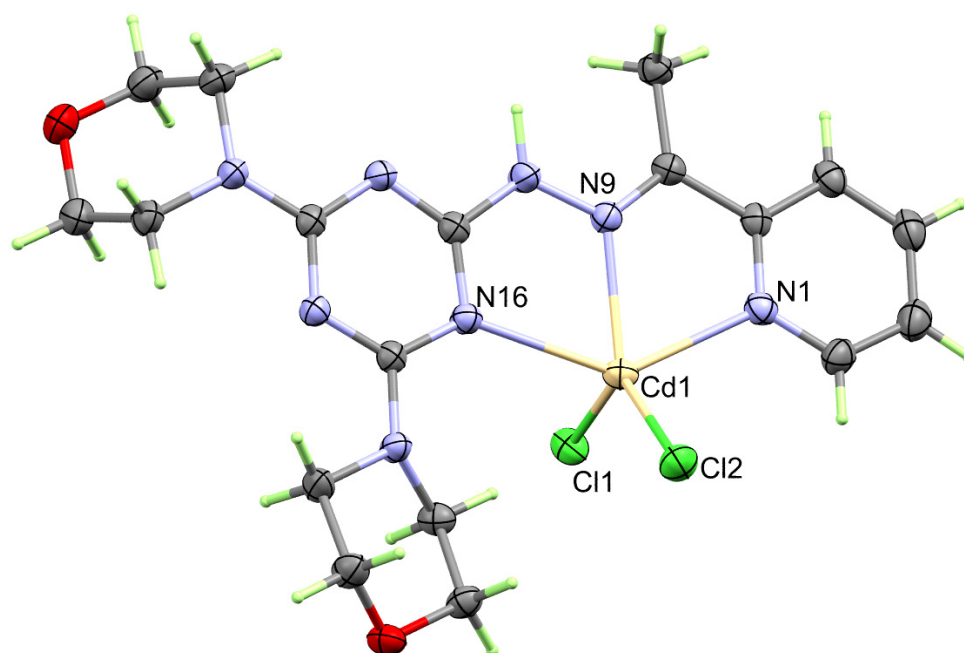


Figure 1. Structure of the coordination sphere of the $[\text{Cd}(\text{DMPT})\text{Cl}_2]$ (**6**) complex.

In the neutral coordination sphere $[\text{Cd}(\text{DMPT})\text{Cl}_2]$ of complex **6**, the Cd(II) is penta-coordinated with one DMPT ligand unit as a neutral tridentate NNN-chelate via the pyridine, hydrazone, and one of the *s*-triazine N-atoms. The Cd1-N1, Cd1-N9, and Cd1-N16 distances are 2.387(2), 2.296(2), and 2.491(2) Å, respectively. The bite angles N9-Cd1-N1 and N9-Cd1-N16 of the DMPT ligand are determined to be 68.31(8) and 69.97(7)°, respectively (Table 2). In addition, the Cd(II) is coordinated with two chloride ions, Cl1 and Cl2, where the Cd to Cl distances are 2.4302(7) and 2.4243(7), respectively, while the Cl1-Cd1-Cl2 angle is 122.73(3)°. Hence, the coordination environment of **1** has a distorted CdN_3Cl_2 penta-

coordination sphere. The Addison τ_5 parameter is used to describe the distortion in the CdN_3Cl_2 penta-coordination sphere. The Addison equation: $\tau_5 = -0.01667\alpha + 0.01667\beta$ gave τ_5 value of 0.09, where α and β are the bond angles N9-Cd1-Cl2 (132.38°) and N1-Cd1-N16 (138.02°), respectively. Hence, the CdN_3Cl_2 penta-coordination sphere is closer to a slightly distorted square pyramid [30,31]. The τ_5 values for the $[\text{Mn}(\text{DMPT})\text{Cl}_2]$ and $[\text{Cu}(\text{DMPT})\text{Cl}_2]$ complexes are significantly higher. In these cases, the τ_5 values were calculated to be 0.332 and 0.235, respectively, indicating more distortion from the ideal square planar configuration around the pentacoordinated Mn(II) and Cu(II) ions than Cd(II). Also, the metal-to-nitrogen distances are determined to be 2.264(2), 2.183(1), and 2.428(1) Å, respectively, in case of the $[\text{Mn}(\text{DMPT})\text{Cl}_2]$ complex while 2.031(4), 1.957(4), and 2.083(4) Å, respectively, in the $[\text{Cu}(\text{DMPT})\text{Cl}_2]$ complex. Also, the bite angles in the $[\text{Mn}(\text{DMPT})\text{Cl}_2]$ complex are $71.29(5)$ and $71.82(5)^\circ$, respectively, while for the $[\text{Cu}(\text{DMPT})\text{Cl}_2]$ complex, the respective values are $78.184(15)$ and $80.142(15)^\circ$, respectively. It is clear that the difference in the geometrical parameters around the coordination sphere of the metal ion is mainly related to the larger size of the Cd(II) compared to the Mn(II) and Cu(II) ions [19].

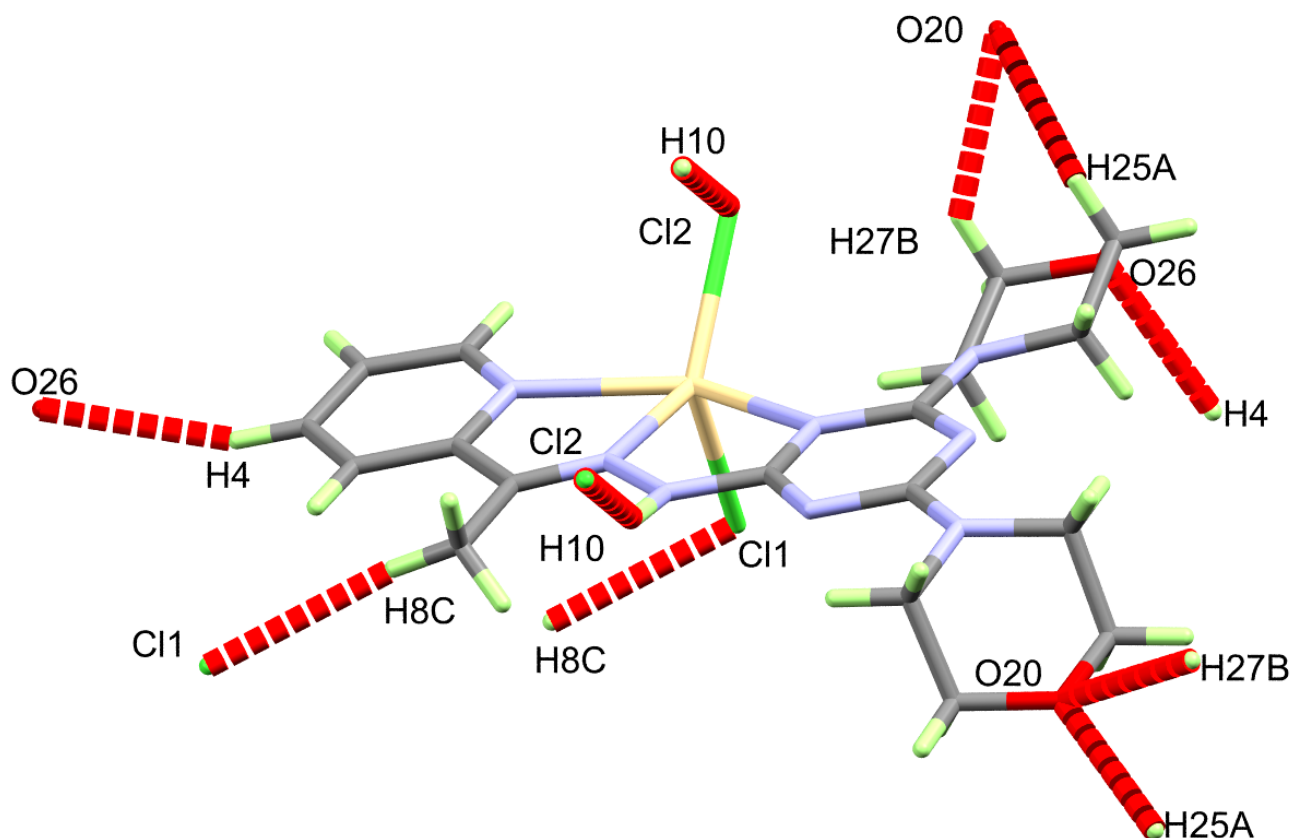
Table 2. Bond distances and angles (Å and $^\circ$) for the coordination environment of complexes 6 and 7.

Bond	Distance	Bond	Distance
Complex 6		Complex 7	
Cd1-Cl1	2.4302(7)	Zn1-Cl1	2.2402(4)
Cd1-Cl2	2.4243(7)	Zn1-Cl2	2.2307(5)
Cd1-N1	2.387(2)	Zn1-N1	2.1481(13)
Cd1-N9	2.296(2)	Zn1-N9	2.0822(12)
Cd1-N16	2.491(2)	Zn1-N12	2.563(13)
Bonds	Angle	Bonds	Angle
Cl1-Cd1-N16	97.79(5)	Cl1-Zn1-N12	98.27(3)
Cl2-Cd1-Cl1	122.73(3)	Cl2-Zn1-Cl1	121.506(18)
Cl2-Cd1-N16	103.34(5)	Cl2-Zn1-N12	95.71(3)
N1-Cd1-Cl1	97.07(6)	N1-Zn1-Cl1	99.45(3)
N1-Cd1-Cl2	101.03(6)	N1-Zn1-Cl2	98.42(3)
N1-Cd1-N16	138.02(7)	N1-Zn1-N12	146.99(5)
N9-Cd1-Cl1	104.82(6)	N9-Zn1-Cl1	122.10(4)
N9-Cd1-Cl2	132.38(6)	N9-Zn1-Cl2	116.21(4)
N9-Cd1-N1	68.31(8)	N9-Zn1-N1	75.73(5)
N9-Cd1-N16	69.97(7)	N9-Zn1-N12	71.26(4)

The supramolecular structure of the $[\text{Cd}(\text{DMPT})\text{Cl}_2]$ complex is controlled by a number of O...H and Cl...H interactions. Information regarding these contacts is given in Table 3 and shown in Figure 2. It is clear that the O20 and O26 from the morpholine moieties, as well as the coordinate chloride ions Cl1 and Cl2, are the hydrogen bond acceptor sites. On the other hand, all the hydrogen bond donors belong to C-H bonds. Hence, the resulting C-H...O and C-H...Cl interactions belong to weak non-classical hydrogen bonds. The donor-acceptor distances for the C-H...O interactions range from 3.310(3) Å (C27-H27B...O20) to 3.502(3) Å (C4-H4...O26). For the C8-H8C...Cl1, the donor-acceptor distance is 3.685(3) Å. The most important hydrogen bond contact is N10-H10...Cl2. The corresponding hydrogen-acceptor and donor-acceptor distances are 2.530(15) and 3.379(2) Å, respectively. The packing scheme of the $[\text{Cd}(\text{DMPT})\text{Cl}_2]$ complex via the C-H...Cl, C-H...O and N-H...Cl interactions is shown in Figure 3. In the case of the structurally related $[\text{Mn}(\text{DMPT})\text{Cl}_2]$ complex, the corresponding donor-to-acceptor values are 3.635(2), 3.438(2), and 3.554(2)-3.635(2) Å, respectively [19].

Table 3. Hydrogen bond geometric parameters in the [Cd(DMPT)Cl₂] (1) complex.

D-H...A	D-H	H...A	D...A	D-H...A	Symm. Code
N10-H10...Cl2	0.976(9)	2.530(15)	3.379(2)	145(2)	$1-x, 1-y, 1-z$
C4-H4...O26	0.95	2.6	3.502(3)	159	$-1/2+x, 3/2-y, 1/2+z$
C8-H8C...Cl1	0.98	2.74	3.685(3)	162	$1-x, 2-y, 1-z$
C25-H25A...O20	0.99	2.57	3.347(4)	135	$1/2+x, 1/2-y, 1/2+z$
C27-H27B...O20	0.99	2.53	3.310(3)	136	$1/2+x, 1/2-y, 1/2+z$

**Figure 2.** Intermolecular contacts in the [Cd(DMPT)Cl₂] (6) complex.

The structure of the coordination environment of the [Zn(DMPT)Cl₂] complex 7 is very similar to the Cd(II) analogue 6. Its X-ray structure is presented in Figure 4. Also, it crystallized in the monoclinic system and the $P2_1/c$ space group. The unit cell parameters are $a = 11.3735(14)$ Å, $b = 13.8707(13)$ Å, $c = 14.9956(16)$ Å and $\beta = 111.646(2)^\circ$. The asymmetric formula is [Zn(DMPT)Cl₂] and $z = 4$. The unit cell volume is slightly less ($2198.9(4)$ Å³) than complex 6, as is the calculated density (1.573 mg/m³).

Also, Zn(II) is coordinated with one tridentate DMPT ligand as a tridentate ligand via the pyridine, hydrazone, and *s*-triazine N-atoms. The order of the Zn-N distance is: $\text{Zn-N}_{(\text{hydrazone})} < \text{Zn-N}_{(\text{pyridine})} < \text{Zn-N}_{(\text{s-triazine})}$, where the corresponding Zn-N distances are $2.0822(12)$, $2.1481(13)$, and $2.563(13)$ Å, respectively, which is the same order as in 6. The bite angles of the DMPT ligand are slightly larger than found in 1. This fact is possibly attributed to the different sizes of the Zn(II) and Cd(II) central metal ions. The N9-Zn1-N1 and N9-Zn1-N12 bite angles are $75.73(5)$ and $71.26(4)^\circ$, respectively. The Zn-Cl1 and Zn-Cl2 distances are determined to be $2.2402(4)$ and $2.2307(5)$ Å, respectively, while the Cl1-Zn1-Cl2 angle is $121.506(18)^\circ$. Hence, the coordination sphere of 7 has a distorted ZnN₃Cl₂ penta-coordination environment. The Addison τ_5 parameter is used to describe the distortion in the CdN₃Cl₂ penta-coordination sphere. The Addison equation: $\tau_5 = -0.01667\alpha + 0.01667\beta$ gave τ_5 value of 0.41, where α and β are the bond angles N9-Zn1-Cl1 ($122.10(4)^\circ$) and

N1-Zn1-N12 ($146.99(5)^\circ$), respectively. Unlike **6**, the ZnN_3Cl_2 coordination environment is highly distorted and located intermediately between the trigonal bipyramidal and square pyramids [30,31]. In this case, the results are comparable with those of the structurally related $[\text{Mn}(\text{DMPT})\text{Cl}_2]$ and $[\text{Cu}(\text{DMPT})\text{Cl}_2]$ complexes [19].

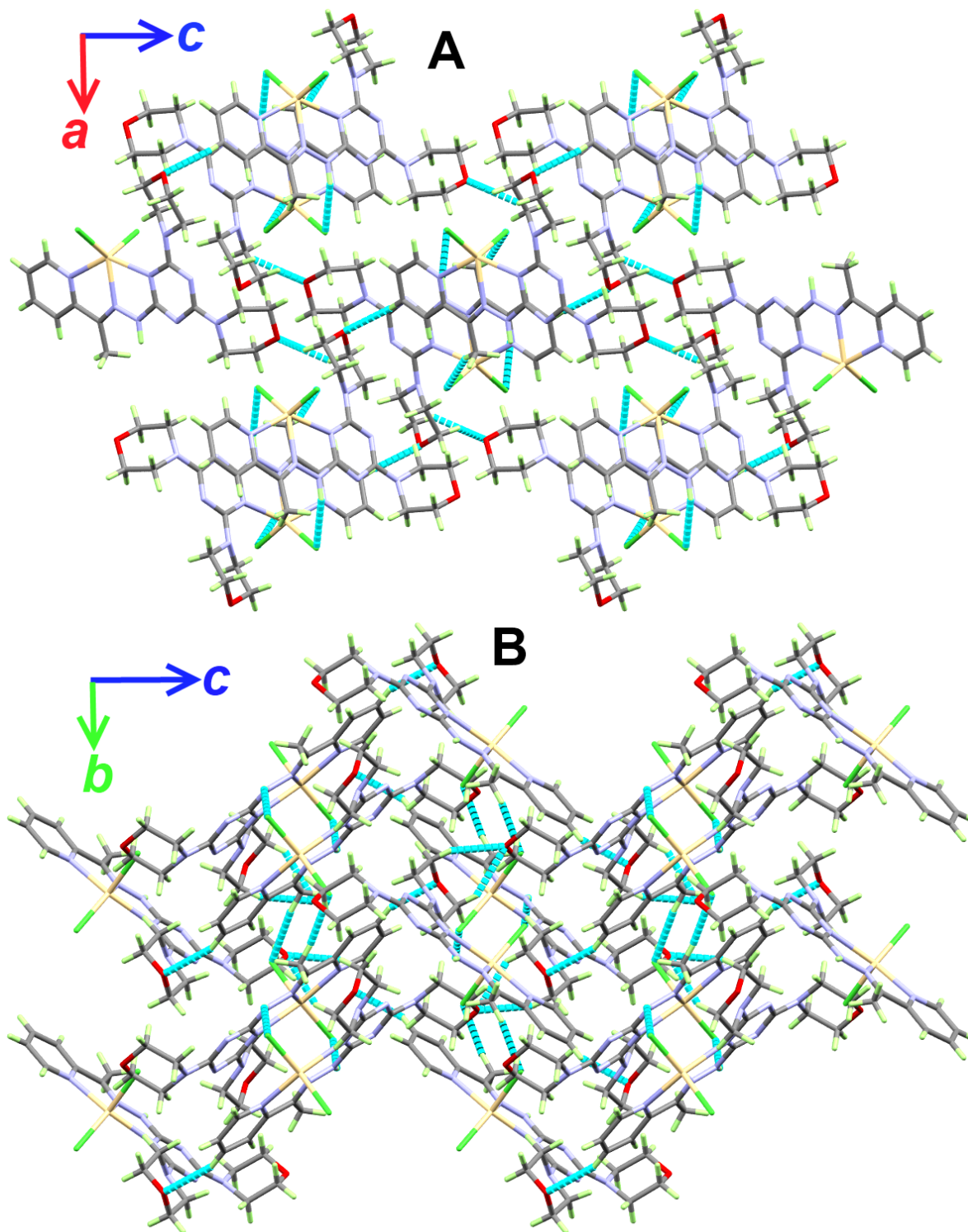


Figure 3. Packing views showing the hydrogen bonds along *ac* (A) and *bc* (B) planes in the $[\text{Cd}(\text{DMPT})\text{Cl}_2]$ (**6**) complex.

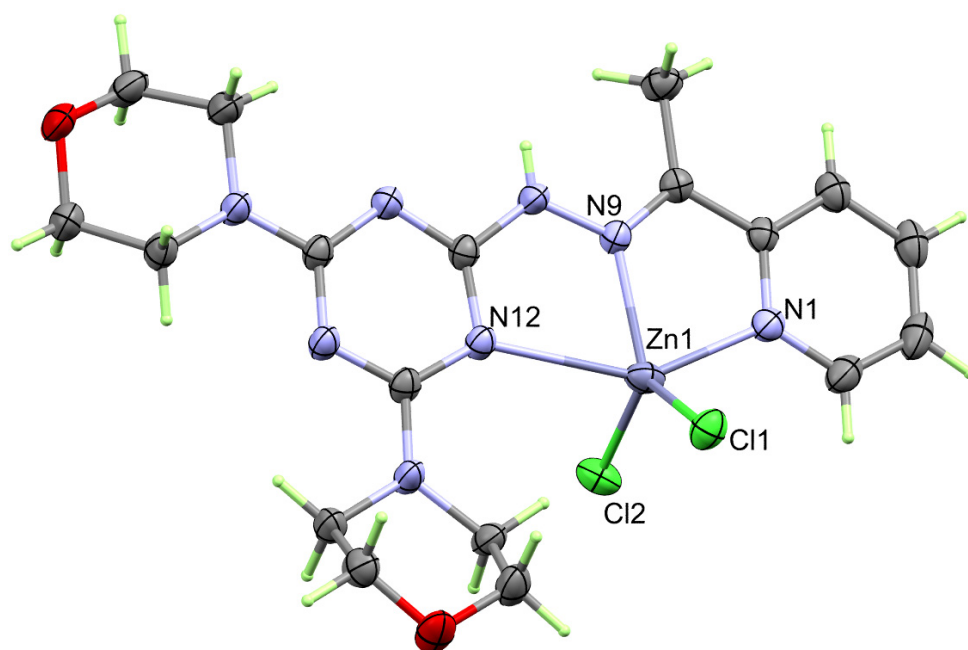


Figure 4. Structure of the $[\text{Zn}(\text{DMPT})\text{Cl}_2]$ (7) complex.

Similar to 6, the supramolecular structure of the $[\text{Zn}(\text{DMPT})\text{Cl}_2]$ complex 7 is controlled by O...H and Cl...H interactions (Table 4). These intermolecular contacts are presented in Figure 5. The most important N10-H10...Cl1 hydrogen bond has hydrogen-acceptor and donor-acceptor distances of 2.74(2) and 3.4417(16) Å, respectively. The other intermolecular interactions belong to the C-H...O and C-H...Cl interactions. The shortest donor-acceptor distances are 3.380(2) Å (C18-H18B...O26) and 3.6063(17) Å (C8-H8C...Cl2), respectively. A view of the packing scheme is shown in Figure 6.

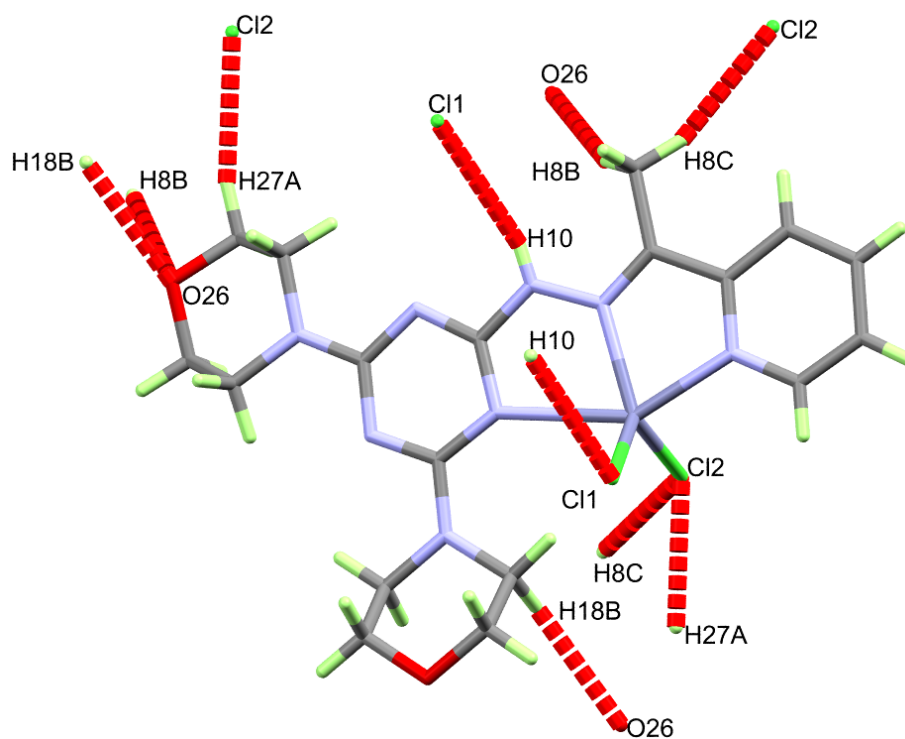
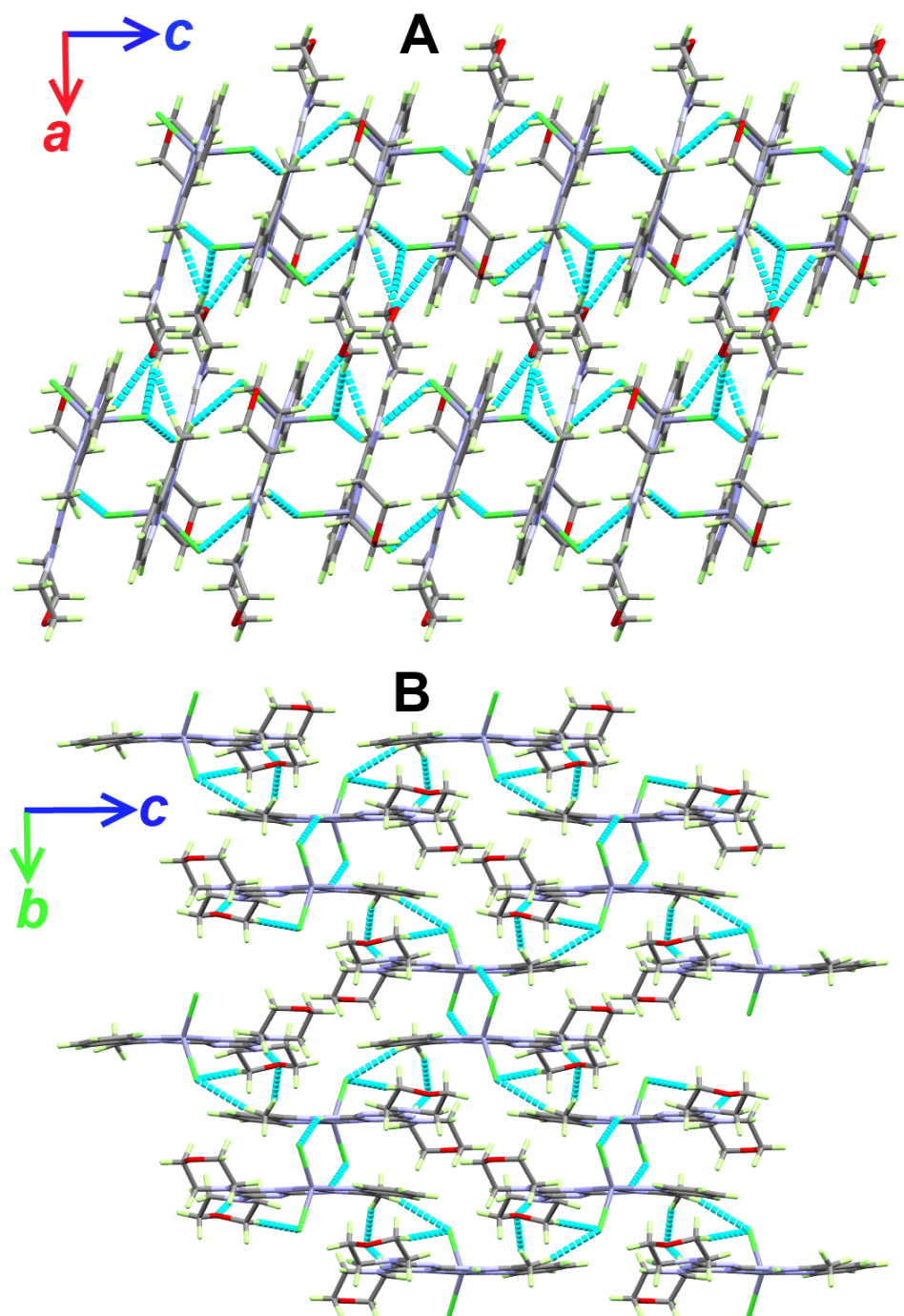


Figure 5. Intermolecular contacts in the $[\text{Zn}(\text{DMPT})\text{Cl}_2]$ (7) complex.

Table 4. Hydrogen bond geometric parameters in the $[\text{Zn}(\text{DMPT})\text{Cl}_2]$ (7) complex.

D-H...A	D-H	H...A	D...A	D-H...A	Symm. Code
N10-H10...Cl1	0.76(2)	2.74(2)	3.4417(16)	155.3(17)	$1 - x, 1 - y, 1 - z$
C8-H8B...O26	0.98	2.56	3.500(2)	160	$2 - x, 1/2 + y, 3/2 - z$
C8-H8C...Cl2	0.98	2.7	3.6063(17)	154	$1 - x, 1/2 + y, 3/2 - z$
C18-H18B...O26	0.99	2.58	3.380(2)	137	$-1 + x, y, z$
C27-H27A...Cl2	0.99	2.68	3.6397(18)	165	$1 + x, y, z$

**Figure 6.** Packing views showing the hydrogen bonds along ac (A) and bc (B) planes in the $[\text{Zn}(\text{DMPT})\text{Cl}_2]$ (7) complex.

3.3. Analysis of Molecular Packing

Self-assembly of small groups or ions is driven by many forces that hold these fragments within the crystal structure in order to maintain optimum conditions for crystal stability. These interactions include hydrogen bonding, π - π stacking, C-H... π , anion... π interactions, and others. Hirshfeld analysis is important not only to inspect these intermolecular interactions but also to calculate their percentages. Different Hirshfeld surfaces for the [Cd(DMPT)Cl₂] complex (**6**) are shown in Figure 7. The different red spots present on the d_{norm} map indicated the presence of significant short contacts, which have shorter distances than the sum of the van der Waals radii sum of the interacting atoms. These red spots are related to the Cl...H, O...H, and C...H interactions, which are labeled on the d_{norm} map by letters A to C for clarity. A summary of all short contacts along with their distances is given in Table 5. The O20...H27B (2.462 Å), O20...H25A (2.505 Å), and O26...H4 (2.473 Å) are the shortest O...H interactions. Regarding Cl...H interactions, the Cl1...H3 (2.725 Å), Cl1...H8C (2.643 Å), Cl2...H5 (2.715 Å), Cl1...H24A (2.814 Å), and Cl2...H10 (2.503 Å) are the shortest, while the Cl3...H25B is the shortest C...H contact with an interaction distance of 2.750 Å. The shape index and curvedness maps show no clear evidence about the presence of π - π stacking interactions (Figure S4; Supplementary Data).

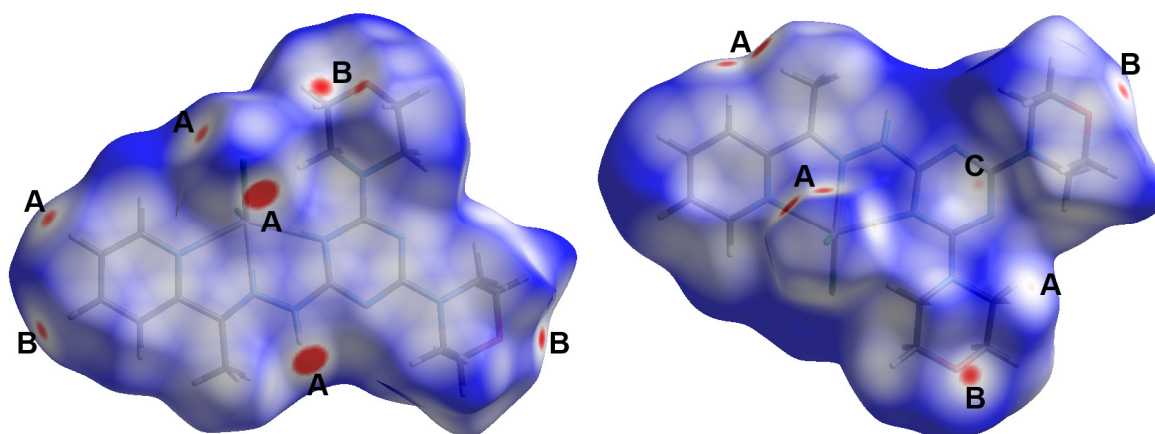


Figure 7. Hirshfeld d_{norm} surfaces for the [Cd(DMPT)Cl₂] complex (**6**). The shape index and curvedness maps are shown in Figure S4 (Supplementary Data).

Table 5. The short intermolecular interactions in the [Cd(DMPT)Cl₂] complex (**6**).

Contact	Distance	Contact	Distance
[Cd(DMPT)Cl ₂]; 6			
O20...H27b	2.462	Cl2...H5	2.715
O20...H25a	2.505	Cl1...H24a	2.814
O26...H4	2.473	Cl2...H10	2.503
Cl1...H3	2.725	Cl3...H25b	2.750
Cl1...H8C	2.643		
[Zn(DMPT)Cl ₂]; 7			
Cl3...H8A	2.721	Cl2...H8C	2.609
O26...H8B	2.468	Cl2...H22B	2.832
O26...H18B	2.517	Cl1...H10	2.513
Cl2...H27A	2.568	N12...H8A	2.576

Also, the Hirshfeld surface analysis of the [Cd(DMPT)Cl₂] complex gave the percentage of all contacts that occurred in its crystal structure. The intermolecular contacts in the crystal structure of **1**, along with their percentages, are presented in Figure 8. The percentages of the Cl...H, O...H, and C...H interactions are 20.9, 9.1, and 8.7%, respectively. The most major intermolecular interaction in the crystal structure of **6** is the hydrogen-

hydrogen interactions, which contributed 45.5% of the total contacts in **6**. Other minor and less important contacts, such as N...H (7.0%), C...N (3.9%), N...N (2.0%), and C...C (1.7%), have less significance in the molecular packing of this complex.

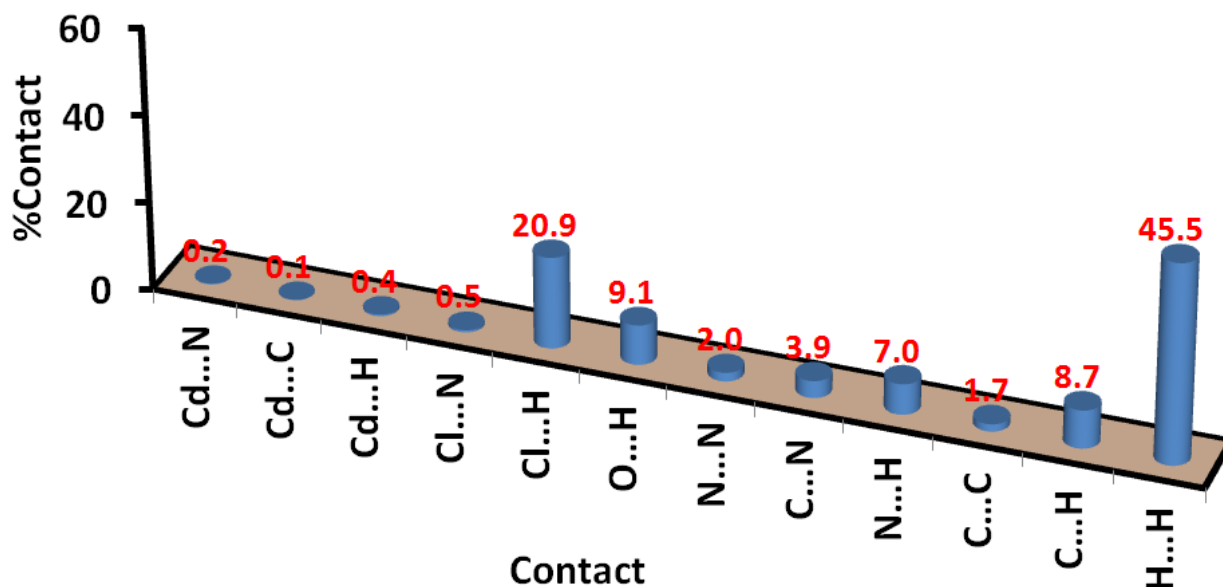


Figure 8. Intermolecular interactions in [Cd(DMPT)Cl₂] (**6**).

Decomposition analysis of the fingerprint plots, such as those shown in Figure 9, not only gave the percentage of all possible contacts in the crystal structure but also gave clear evidence on the important contacts. The fingerprint plots of the Cl...H, O...H, and C...H interactions appeared as sharp spikes, leaving no doubt that these interactions occur at short distances and are considered important.

On the other hand, Hirshfeld surfaces for the [Zn(DMPT)Cl₂] complex (**7**) are shown in Figure 10. In this complex, there are four types of short contacts, which are the Cl...H (**A**), O...H (**B**), C...H (**C**), and C...H (**D**) interactions. A summary of these short contacts is listed in Table 5. The Cl2...H27A (2.568 Å), Cl2...H8C (2.609 Å), Cl2...H22B (2.832 Å), and Cl1...H10 are the shortest Cl...H interactions. There are two short O...H interactions, which are the O26...H8B (2.468 Å) and O26...H18B (2.517 Å), in addition to the short Cl3...H8A (2.721 Å) contact. All these contacts are comparable to those detected in complex **6**. Similarly, it has similar interaction distances to those in **6**. A new contact was observed that is not found in complexes; it is the N12...H8A interaction, which has an interaction distance of 2.576 Å. All these contacts appeared in the d_{norm} as red spots, indicating their significance.

In Figure 11, a list of all possible intermolecular interactions in the crystal structure of **7** is shown. Similar to complex **6**, the H...H contacts are the most dominant. Their percentages were calculated to be 46.4%. In addition, the short Cl...H, O...H, C...H, and N...H contacts contributed significantly to the molecular packing by 20.3, 9.0, 7.0, and 8.4%, respectively. The other contacts presented in this figure are found to be of less importance. Also, the shape index and curvedness maps show the absence of π - π stacking interactions (Figure S5; Supplementary Data).

The fingerprint plots' decomposition not only gave the percentage of all possible contacts in the crystal structure of **7** but also indicated very well the importance of the Cl...H, O...H, C...H, and N...H contacts (Figure 12). All these contacts appeared as spikes, indicating their importance, which is in accordance with the d_{norm} map analysis.

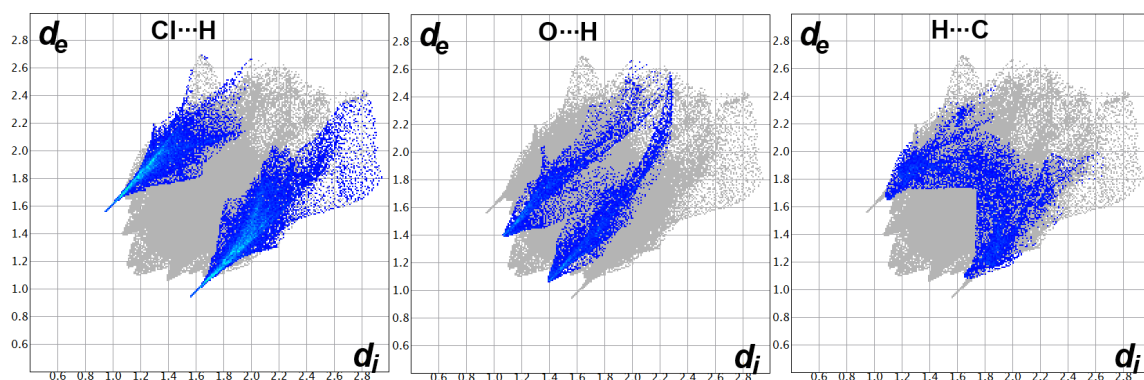


Figure 9. Fingerprint plots for the important interactions in $[\text{Cd}(\text{DMPT})\text{Cl}_2]$ (6).

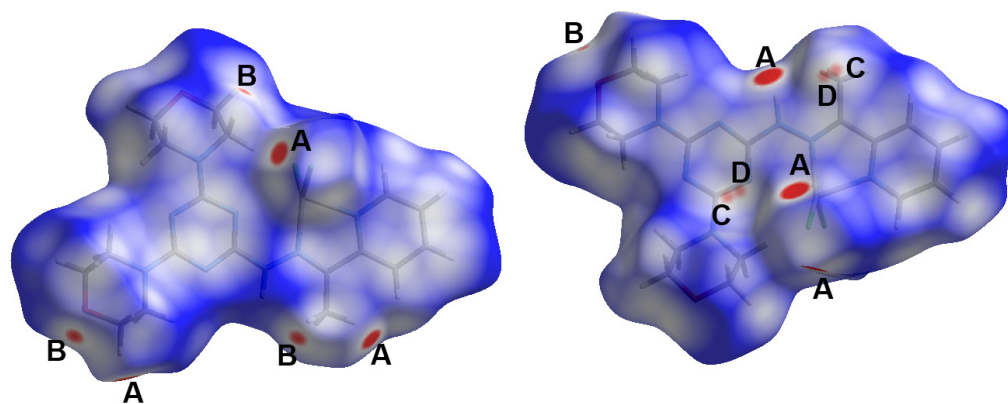


Figure 10. Hirshfeld surfaces for $[\text{Zn}(\text{DMPT})\text{Cl}_2]$ (7). The shape index and curvedness maps are shown in Figure S5 (Supplementary Data).

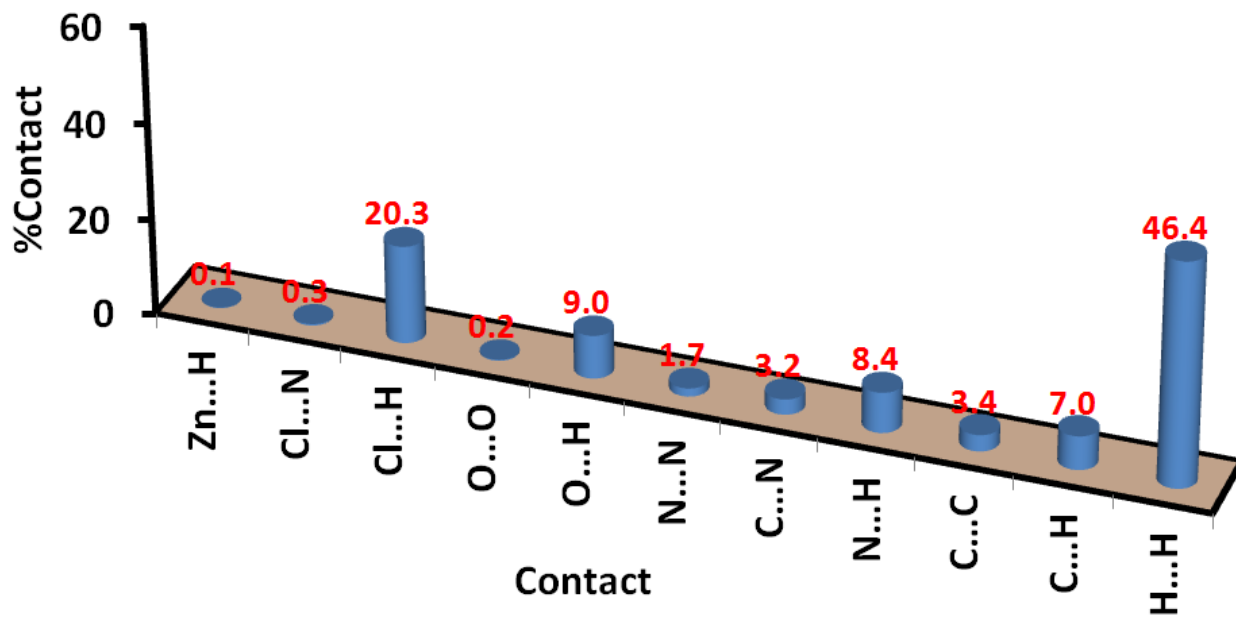


Figure 11. Intermolecular interactions in $[\text{Zn}(\text{DMPT})\text{Cl}_2]$ (7).

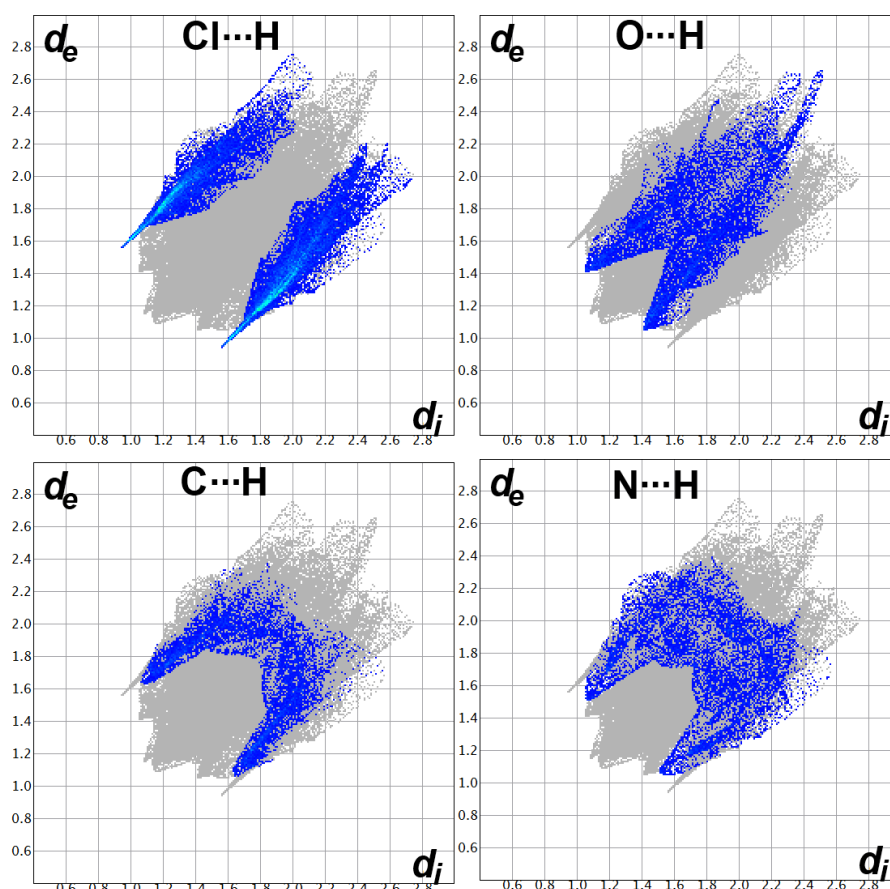


Figure 12. Fingerprint plots for the important interactions in $[\text{Zn}(\text{DMPT})\text{Cl}_2]$ (7).

4. Conclusions

The X-ray crystallographic analyses of the $[\text{Cd}(\text{DMPT})\text{Cl}_2]$ (6) and $[\text{Zn}(\text{DMPT})\text{Cl}_2]$ (7) complexes were presented. Both complexes have similar penta-coordination environments. The CdN_3Cl_2 coordination environment is close to a distorted square pyramidal configuration, while the ZnN_3Cl_2 coordination environment is an intermediate between the trigonal bipyramidal and square pyramids. Hirshfeld surface analysis of 6 revealed the importance of contacts such as $\text{Cl} \cdots \text{H}$ (20.9%), $\text{O} \cdots \text{H}$ (9.1%), and $\text{C} \cdots \text{H}$ (8.7%) in the molecular packing. Also, the $\text{Cl} \cdots \text{H}$ (20.3%), $\text{O} \cdots \text{H}$ (9.0%), $\text{C} \cdots \text{H}$ (7.0%), and $\text{N} \cdots \text{H}$ (8.4%) contacts are the most significant in 7. The hydrogen-hydrogen interactions are the most dominant and contributed to almost half of the total interactions. The percentages of the $\text{H} \cdots \text{H}$ interactions are 45.5 and 46.4% for complexes 6 and 7, respectively. We are inspired to conduct additional research on this class of ligands in order to further shed light on the effect of metal ion type on their coordination behavior.

Supplementary Materials: The following supporting information can be downloaded at: <https://www.mdpi.com/article/10.3390/cryst13081232/s1>, Method S1. Crystal structure determination; Figure S1 FTIR spectra of DMPT; Figure S2 FTIR spectra of 6; Figure S3 FTIR spectra of 7; Figure S4 The shape index and curvedness maps for $[\text{Cd}(\text{DMPT})\text{Cl}_2]$ (6); Figure S5 The shape index and curvedness maps for $[\text{Zn}(\text{DMPT})\text{Cl}_2]$ (7).

Author Contributions: Conceptualization, M.A.M.A.-Y. and S.M.S.; formal analysis, S.M.S., A.M.Z.S. and J.D.W.; investigation, M.A.M.A.-Y. and S.M.S.; methodology, S.M.S. and A.B.; software, S.M.S., A.M.Z.S. and J.D.W.; Crystallographer, A.M.Z.S. and J.D.W.; supervision, M.A.M.A.-Y., A.B. and S.M.S.; validation, A.E.-F. and A.B.; visualization, A.E.-F.; funding acquisition: A.B.; writing—original draft, S.M.S.; writing—review and editing, M.A.M.A.-Y., A.E.-F. and A.B. All authors have read and agreed to the published version of the manuscript.

Funding: The authors would like to extend their sincere appreciation to the Researchers Supporting Project (RSP2023R64), King Saud University, Riyadh, Saudi Arabia.

Data Availability Statement: Not applicable.

Acknowledgments: The authors would like to extend their sincere appreciation to the Researchers Supporting Project (RSP2023R64), King Saud University, Riyadh, Saudi Arabia.

Conflicts of Interest: The authors declare no conflict of interest.

References

1. Barakat, A.; El-Faham, A.; Haukka, M.; Al-Majid, A.M.; Soliman, S.M. s-Triazine pincer ligands: Synthesis of their metal complexes, coordination behavior, and applications. *Appl. Organomet. Chem.* **2021**, *35*, e6317. [[CrossRef](#)]
2. Memon, Q.S.; Memon, N.; Mallah, A.; Soomro, R.; Khuhawar, Y.M. Schiff bases as chelating reagents for metal ions analysis. *Curr. Anal. Chem.* **2014**, *10*, 393–417. [[CrossRef](#)]
3. Abu-Dief, A.M.; Mohamed, I.M.A. A review on versatile applications of transition metal complexes incorporating Schiff bases. *Beni-Suef Univ. J. Appl.* **2015**, *4*, 119–133. [[CrossRef](#)] [[PubMed](#)]
4. Al Zoubi, W. Solvent extraction of metal ions by use of Schiff bases. *J. Coord. Chem.* **2013**, *66*, 2264–2289. [[CrossRef](#)]
5. Rezaeivala, M.; Keypour, H. Schiff base and non-Schiff base macrocyclic ligands and complexes incorporating the pyridine moiety—The first 50 years. *Coord. Chem. Rev.* **2014**, *280*, 203–253. [[CrossRef](#)]
6. Liu, X.; Hamon, J.R. Recent developments in penta-, hexa- and heptadentate Schiff base ligands and their metal complexes. *Coord. Chem. Rev.* **2019**, *389*, 94–118. [[CrossRef](#)]
7. Saghatforoush, L.; Khoshtarkib, Z.; Keypour, H.; Hakimi, M. Mononuclear, tetranuclear and polymeric cadmium(II) complexes with the 3,6-bis(2-pyridyl)-1,2,4,5-tetrazine ligand: Synthesis, crystal structure, spectroscopic and DFT studies. *Polyhedron* **2016**, *119*, 160–174. [[CrossRef](#)]
8. Mlowe, S.; Lewis, D.J.; Malik, M.A.; Raftery, J.; Mubofu, E.B.; O'Brien, P.; Revaprasadu, N. Bis(piperidinedithiocarbamate)-pyridinecadmium(ii) as a single-source precursor for the synthesis of CdS nanoparticles and aerosol-assisted chemical vapour deposition (AACVD) of CdS thin films. *New J. Chem.* **2014**, *38*, 6073–6080. [[CrossRef](#)]
9. Bjelogrić, S.; Todorović, T.; Bacchi, A.; Zec, M.; Sladić, D.; Srdić-Rajić, T.; Radanović, D.; Radulović, S.; Pelizzi, G.; Anđelković, K. Synthesis, structure and characterization of novel Cd(II) and Zn(II) complexes with the condensation product of 2-formylpyridine and selenosemicarbazide Antiproliferative activity of the synthesized complexes and related selenosemicarbazone complexes. *J. Inorg. Biochem.* **2010**, *104*, 673–682. [[CrossRef](#)]
10. Soliman, S.M.; El-Faham, A. Synthesis and structure diversity of high coordination number Cd(II) complexes of large s-triazine bis-Schiff base pincer chelate. *Inorg. Chim. Acta* **2019**, *488*, 131–140. [[CrossRef](#)]
11. Filipović, N.R.; Bacchi, A.; Lazić, M.; Pelizzi, G.; Radulović, S.; Sladić, D.M.; Todorović, T.R.; Anđelković, K.K. Structure and Cytotoxic Activity Evaluation of a Dinuclear Complex of Cd(II) with N', N'2-bis[(1E)-1-(2-pyridyl)ethylidene]propanedihydrazide. *Inorg. Chem. Commun.* **2008**, *11*, 47–50. [[CrossRef](#)]
12. Ali, M.A.; Mirza, A.H.; Nazimuddin, M.; Rahman, H.; Butcher, R.J. The preparation and characterization of mono- and bischelated cadmium(II) complexes of the di-2-pyridylketone Schiff base of S-methyldithiocarbazate (Hdpksme) and the X-ray crystal structure of the [Cd(dpksme)₂].0.5MeOH complex. *Trans. Met. Chem.* **2002**, *27*, 268–273.
13. Ray, S.; Konar, S.; Jana, A.; Jana, S.; Patra, A.; Chatterjee, S.; Golen, J.A.; Rheingold, A.L.; Mandal, S.S.; Kar, S.K. Three new pseudohalide bridged dinuclear Zn(II), Cd(II) complexes of pyrimidine derived Schiff base ligands: Synthesis, crystal structures and fluorescence studies. *Polyhedron* **2012**, *33*, 82–89. [[CrossRef](#)]
14. Al Rasheed, H.H.; Malebari, A.M.; Dahlous, K.A.; Fayne, D.; El-Faham, A. Synthesis, anti-proliferative activity, and molecular docking study of new series of 1,3-5-triazine Schiff base derivatives. *Molecules* **2020**, *25*, 4065. [[CrossRef](#)]
15. Al-Rasheed, H.H.; Mohammady, S.Z.; Dahlous, K.; Siddiqui, M.R.; El-Faham, A. Synthesis, characterization, thermal stability and kinetics of thermal degradation of novel polymers based-s-triazine Schiff base. *J. Polym. Res.* **2020**, *27*, 10. [[CrossRef](#)]
16. Uysal, Ş.; Kurşunlu, A.N. The Synthesis and characterization of star shaped metal complexes of triazine cored schiff bases: Their thermal decompositions and magnetic moment values. *J. Inorg. Organomet. Polym. Mater.* **2011**, *21*, 291–296. [[CrossRef](#)]
17. Shanmuga kala, R.; Tharmaraj, P.; Sheela, C.D. Synthesis, spectral studies, NLO, and biological studies on metal (II) complexes of s-triazine-based ligand. *Synth. React. Inorg. Met.* **2014**, *44*, 1487–1496. [[CrossRef](#)]
18. Dahlous, K.A.; Alotaibi, A.A.; Dege, N.; El-Faham, A.; Soliman, S.M.; Refaat, H.M. X-ray Structure Analyses and Biological Evaluations of a New Cd (II) Complex with s-Triazine Based Ligand. *Crystals* **2022**, *12*, 861. [[CrossRef](#)]
19. Fathalla, E.M.; Abu-Youssef, M.A.M.; Sharaf, M.M.; El-Faham, A.; Barakat, A.; Badr, A.M.A.; Soliman, S.M.; Slawin, A.M.Z.; Woollins, J.D. Synthesis, Characterizations, Antitumor and Antimicrobial Evaluations of Novel Mn(II) and Cu(II) Complexes with NNN-tridentate s-Triazine-Schiff base Ligand. *Inorg. Chim. Acta* **2023**, *555*, 121586. [[CrossRef](#)]
20. Fathalla, E.M.; Abu-Youssef, M.A.M.; Sharaf, M.M.; El-Faham, A.; Barakat, A.; Haukka, M.; Soliman, S.M. Synthesis, X-ray Structure of Two Hexa-Coordinated Ni(II) Complexes with s-Triazine Hydrazine Schiff Base Ligand. *Inorganics* **2023**, *11*, 222. [[CrossRef](#)]
21. Sheldrick, G.M. A short history of SHELX. *Acta Cryst. A* **2008**, *64*, 112–122. [[CrossRef](#)] [[PubMed](#)]

22. Crane, B.C.; Barwell, N.P.; Gopal, P.; Gopichand, M.; Higgs, T.; James, T.D.; Jones, C.M.; Mackenzie, A.; Mulavisala, K.P.; Paterson, W. Advances in applied supramolecular technologies. *J. Diabetes Sci. Technol.* **2015**, *9*, 751–761. [[CrossRef](#)] [[PubMed](#)]
23. De Silva, A.P.; Sandanayake, K.R.A.S. Fluorescent PET (photo-induced electron transfer) sensors for alkali metal ions with improved selectivity against protons and with predictable binding constants. *J. Chem. Soc.* **1989**, *16*, 1183–1185. [[CrossRef](#)]
24. Nakahata, M.; Mori, S.; Takashima, Y.; Yamaguchi, H.; Harada, A. Self-Healing Materials Formed by Cross-Linked Polyrotaxanes with Reversible Bonds. *Chem* **2016**, *1*, 766–775. [[CrossRef](#)]
25. Wu, J.R.; Cai, L.H.; Weitz, D.A. Tough Self-Healing Elastomers by Molecular Enforced Integration of Covalent and Reversible Networks. *Adv. Mater.* **2017**, *29*, 1702616. [[CrossRef](#)]
26. Jaglenieć, D.; Dobrzycki, Ł.; Karbarz, M.; Romański, J. Ion-pair induced supramolecular assembly formation for selective extraction and sensing of potassium sulfate. *J. Chem. Sci.* **2019**, *10*, 9542–9547. [[CrossRef](#)]
27. Williams, N.J.; Seipp, C.A.; Garrabrant, K.A.; Custelcean, R.; Holguin, E.; Keum, J.K.; Ellis, R.J.; Moyer, B.A. Surprisingly selective sulfate extraction by a simple monofunctional di(imino)guanidinium micelle-forming anion receptor. *Chem. Commun.* **2018**, *54*, 10048–10051. [[CrossRef](#)]
28. Williams, G.T.; Haynes, C.J.E.; Fares, M.; Caltagirone, C.; Hiscock, J.R.; Gale, P.A. Advances in applied supramolecular technologies. *Chem. Soc. Rev.* **2021**, *50*, 2737. [[CrossRef](#)]
29. Spackman, P.R.; Turner, M.J.; McKinnon, J.J.; Wolff, S.K.; Grimwood, D.J.; Jayatilaka, D.; Spackman, M.A. Crystal Explorer: A program for Hirshfeld surface analysis, visualization and quantitative analysis of molecular crystals. *J. Appl. Crystallogr.* **2021**, *27*, 1006–1011. [[CrossRef](#)]
30. Addison, A.W.; Rao, N.T.; Reedijk, J.; van Rijn, J.; Verschoor, G.C. Synthesis, structure, and spectroscopic properties of copper(II) compounds containing nitrogen–sulphur donor ligands; the crystal and molecular structure of aqua [1,7-bis(N-methylbenzimidazol-2'-yl)-2,6-dithiaheptane]copper(II) perchlorate. *J. Chem. Soc. Dalton Trans.* **1984**, *7*, 1349–1356. [[CrossRef](#)]
31. Kepert, D.L. *Inorganic Stereochemistry, Inorganic Chemistry Concepts*; Springer: Berlin/Heidelberg, Germany, 1982.

Disclaimer/Publisher's Note: The statements, opinions and data contained in all publications are solely those of the individual author(s) and contributor(s) and not of MDPI and/or the editor(s). MDPI and/or the editor(s) disclaim responsibility for any injury to people or property resulting from any ideas, methods, instructions or products referred to in the content.